

# Electrochemical study of cerium(IV) in the presence of ethylenediaminetetraacetic acid (EDTA) and diethylenetriaminepentaacetate (DTPA) ligands

P. Modiba · A. M. Crouch

Received: 28 September 2007 / Revised: 27 March 2008 / Accepted: 28 March 2008 / Published online: 11 April 2008  
© Springer Science+Business Media B.V. 2008

**Abstract** The electrochemical behaviour of the complexation of cerium(IV) with EDTA and DTPA was studied using both cyclic voltammetry (CV) and rotating disc electrode (RDE). The Ce(IV)–DTPA complex at various scan rates gave a linear correlation between the peak potential ( $E_p$ ) and square root of scan rate, showing that the kinetics of the overall process was controlled by mass transport. However, when the EDTA ligand was added to the Ce(IV) there was no specific change to the potential peak, i.e. the Ce(IV)–EDTA complex has the same redox potential as the Ce(IV)/(III) couple. Kinetic parameters such as potential, limiting current, diffusion coefficients, transfer coefficient and rate constants were studied. The results from RDE experiments confirmed that the parameters measured by CV are similar under hydrodynamic conditions and can be used to determine the kinetic parameters of the redox couples. The use of DTPA as a ligand for complexation of Ce(IV) gives more favourable results compared to the Ce–(EDTA) complex reported previously. The results of kinetic studies of Ce(IV)–DTPA complex shows promise as an electrolyte for redox flow battery.

**Keywords** Cyclic voltammetry · Rotating disc electrode · Ce(IV)–EDTA · Ce(IV)–DTPA · Redox flow battery

## 1 Introduction

The search for stable redox systems for use in redox flow batteries (RFBs) has been an active field of research for the

past few years [1–7]. A typical battery makes use of two fully soluble redox couples, and consists of stacks, electrolytes, pumps and tanks. The storage capacity is determined by the electrolyte concentration and the size of the battery cells.

The first study of redox flow batteries was reported by Thaller [2] who used  $\text{Fe}^{2+}/\text{Fe}^{3+}$  and  $\text{Cr}^{2+}/\text{Cr}^{3+}$  redox couples for the redox flow cell energy storage systems. Later reports [3, 4] described a multiplicity of redox couple flow batteries ( $\text{Fe}^{2+}/\text{Fe}^{3+}$  and  $\text{V}^{4+}/\text{V}^{5+}$ ), ( $\text{Fe}^{2+}/\text{Fe}^{3+}$  and  $\text{Ti}^{+3}/\text{TiO}^{+2}$ ), ( $\text{Fe}^{2+}/\text{Fe}^{3+}$  and  $\text{V}^{2+}/\text{VO}^{2+}$ ), ( $\text{Cr}^{2+}/\text{Cr}^{3+}$  and  $\text{Cu}(\text{NH}_3)_2^{+1}/\text{Cu}(\text{NH}_3)_4^{+2}$ ) and ( $\text{V}^{2+}/\text{VO}^{2+}$   $\text{Fe}(\text{O}_3)^{-3}/\text{Fe}(\text{O}_3)^{-4}$ ) systems for redox cell development. Reid et al. [5] also tried to use the  $\text{Fe}^{2+}/\text{Fe}^{3+}$  and  $\text{Cr}^{2+}/\text{Cr}^{3+}$  couples in redox flow batteries. All these studies encountered the same problem of poor reversibility and the cross mixing of anolyte and catholyte through the separating membrane because of the use of two separate redox couples in a half cell. The system also suffered from serious efficiency losses, and reduces the life time of expensive membranes. All these problems can be minimized by employing the same element in different oxidation states. In both half cells this approach requires the use of different complexing agents to provide a workable difference in redox potential. Quantities of redox couples based on a single species (all-vanadium, iron, chromium, cerium, and neptunium) have been reported in the literature [6–13].

Recently a lot of attention was focused on the all-vanadium RFB [6, 7, 10, 11] due to its various advantages, where there is no decrease in capacity caused by the cross mixing of the positive electrolyte and negative electrolyte, meaning that there will be no energy efficiency loss during the process. The effect of cross-contamination for All-vanadium RFB does not need catalysts for both electrode reactions, and there is no evolution of hydrogen gas, which needs rebalancing power and additional equipment. Even

P. Modiba · A. M. Crouch (✉)  
Department of Chemistry, University of Stellenbosch, Private  
Bag No. X I, Stellenbosch 7602, South Africa  
e-mail: amc@sun.ac.za

though these qualities exist for all-vanadium redox flow systems the open-circuit voltage for each single cell after full charging is about 1.4 V, which is relatively low. Lui et al. [4] proved that vanadium can be replaced by cerium. Fang et al. [14] investigated the Ce(IV)/Ce(III) couple, which has a standard reduction potential of 1.74 V which is higher than the all-vanadium RFB. Paulenova et al. [15] evaluated the cerium couple in a RFB because of its positive redox potential, and the cell voltage was predicted to be approximately 1.9 V.

The use of the Ce<sup>4+</sup>/Ce<sup>3+</sup> redox couple is attractive for RFB technology because of its large positive redox potential, which should result in a battery with a higher cell voltage and a greater energy storage capacity. Pletcher et al. [16] reported the electrochemical behaviour of the Ce<sup>4+</sup>/Ce<sup>3+</sup> redox couple in aqueous nitrite media and the electrochemistry of the Ce<sup>4+</sup>/Ce<sup>3+</sup> couple in sulphuric acids solution has been widely investigated [17–20].

The kinetics and mechanism of the oxidation of organic compounds by various oxidizing agents have also received considerable attention in the recent years. In particular, the oxidation of different organic compounds using carboxylic acids and alcohol with Ce(IV) has been studied extensively. Abbaspour et al. [18] investigated the electrochemical behaviour of Ce(III) ions in the presence of EDTA, and they determined the kinetic parameters such as transfer coefficient and rate constants for electrocatalytic oxidation of nitrite ion. Glenwith et al. [19] investigated the kinetic study of isotopic exchange reactions between lanthanide ions and lanthanide polyaminopolycarboxylic acid complex ions in aqueous solution for chemical effect of nuclear transformation of Ce–EDTA and Ce–DTPA couples. This work was used as a point of departure to demonstrate the superior performance of the Ce–DTPA complex. A search has revealed that there is no electrochemical study of Ce(IV) in the presence of DTPA as a ligand or complexone for use in redox flow batteries system. In this paper we report the study of Ce(IV) redox system using EDTA or DTPA as a ligand for redox flow batteries. It was also compared to Ce–DTPA and Ce–EDTA system to show that the former system is more promising than the latter in terms of its stability and electron transfer capability. A comparison was also made of similar systems of iron.

## 2 Experimental

### 2.1 Materials and reagents

All reagents were of analytical reagent grade unless stated otherwise. Ethylenediaminetetraacetic acid (EDTA), sulphuric acid, potassium ferricyanide (K<sub>3</sub>Fe(CN)<sub>6</sub>), Potassium Nitrate (KNO<sub>3</sub>) Sodium hydroxide, cerium(IV)

sulphate and diethylenetriaminepentaacetic acid (DTPA) are obtained from Sigma-Aldrich (Steinheim, Germany).

### 2.2 Preparation of Ce(IV)–DTPA and Ce(IV)–EDTA

Cerium(IV) sulphate [Ce(SO<sub>4</sub>)<sub>2</sub>] and Ce(IV)–EDTA were prepared as described in the literature [21]. For preparation of Ce(IV)–DTPA, DTPA was added to replace EDTA as per literature method [21], and dissolved in 1 M H<sub>2</sub>SO<sub>4</sub>. The solution was filtered and poured in a small designed Cyclic Voltammetry glass cell. Deionized water was prepared by passing distilled water through a Millipore (Bedford, MA, USA) Milli Q water purification system.

### 2.3 Preparation of Fe(III)–DTPA and Fe(III)–EDTA

Fe(III)–DTPA and Fe(III)–EDTA were prepared by dissolving potassium ferricyanide (K<sub>3</sub>Fe(CN)<sub>6</sub>) in 0.1 M potassium nitrate (KNO<sub>3</sub>) solution. The specific amount of EDTA and DTPA was added in a separate container to complex with the prepared solution of iron.

### 2.4 Instrumentation

Cyclic Voltammetry (CV) measurements were performed using a BAS 100B voltammetric system. A rotating disc electrochemistry (RDE) stand was used in conjunction with the BAS 100B voltammetric system from Bioanalytical Systems, Inc. West Lafayette, Indiana, USA.

#### 2.4.1 Electrochemical measurements

The electrochemical behaviour of Ce(IV) ion in the presence of EDTA and DTPA was investigated with cyclic voltammetry and rotating disc electrochemistry or hydrodynamic voltammetry techniques. The electrodes used for both CV and RDE experiments include: platinum disc electrode with a diameter of 3 mm as a working electrode, Ag/AgCl as a reference electrode and a platinum wire as a counter electrode. The electrodes were initially hand polished with 600–1200 grit paper. Before each experiment they were then polished with a microcloth using 1, 0.3, and 0.05 μm alumina, followed by rinsing the electrodes with de-ionized water. Thereafter the electrodes were polished with 1 μm diamond polish slurry. The electrodes were rinsed again several times with de-ionized water and methanol to remove polishing residues. The surface activity was confirmed by cyclic voltammograms for K<sub>3</sub>Fe(CN)<sub>6</sub> in 0.1 M KNO<sub>3</sub> solution. The solutions were de-aerated by bubbling with nitrogen before each experiment for 10 min. Analyses were carried out at room temperature at various scan rates of 20–200 mV s<sup>-1</sup>.

### 3 Results and discussions

#### 3.1 Cyclic voltammetry

The cyclic voltammograms for the cerium(IV) sulphate in 1 M sulphuric acid are shown in Fig. 1a and b. Forward scans reveal that the anodic peak associated with the oxidation of  $\text{Ce}^{3+}$  to  $\text{Ce}^{4+}$  occurs at approximately 1020 mV. On the reverse scan, the cathodic peak associated with the reduction of  $\text{Ce}^{4+}$  to  $\text{Ce}^{3+}$  occurs at approximately 1290 mV versus Ag/AgCl. It can be seen in Fig. 1b that the anodic and cathodic peak potential changed slightly with different scan rates. Therefore, the electrochemical process will be quasi-reversible since the separation between the forward and reverse potential peak  $\Delta E_p$  is more than 59 mV, and the potential of the forward peak is independent of the scan rate.

Pletcher et al. [16] reported a larger peak potential separation from the cyclic voltammograms of Ce(III)/Ce(IV)– $\text{H}_2\text{SO}_4$  system obtained at carbon electrodes. A similar study of the Ce(III)/(IV) redox couple by Fang et al. [14] confirmed the irreversible nature of the Ce(III)/(IV) redox couple in the presence of sulphuric acid. Fang et al. also investigated the effect of sulphuric acid concentration on the formal potential of the cerium redox couple.

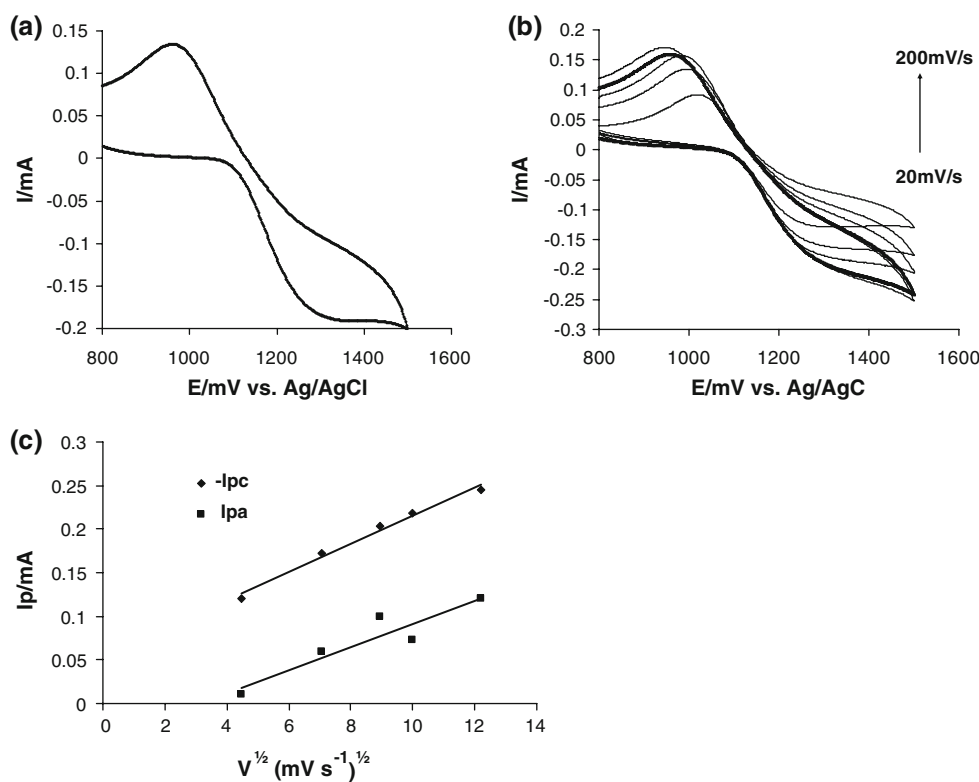
The scan rate dependence of the peak currents and peak potentials in sulphuric acid is reported in Fig. 1c. There is a

linear relationship between peak current and scan rate, indicating a diffusion controlled reaction.

Figure 2a and b shows the voltammograms of Ce(IV) aminocarboxylate complexes in 1 M  $\text{H}_2\text{SO}_4$  solution. The peak potential  $E_{pa}$  and  $E_{pc}$  values are observed at around 1020 mV and 1290 mV. Both the cathodic peak and anodic peak potentials changed slightly with the scan rate as shown in Fig. 2b. Peak splitting was found to increase with increasing scan rate, meaning a larger peak separation was observed and the electrochemical process was irreversible. The redox reaction Ce(III) to Ce(IV) shows a quasi-reversible electrochemical behaviour, Ce(IV)–EDTA illustrate an irreversible behaviour, whereas the Ce(IV)–DTPA complex is quasi-reversible as shown in Fig. 2c. The cathodic peak potential shift towards more negative potential values for the reduction step, the current ratio  $I_{pa}/I_{pc}$  for the Ce(IV)–DTPA complex was found to be 0.84 and the transfer coefficient ( $\alpha$ ) from the Table 1 was found to be 0.42. This ratio and transfer coefficient supports the notion that the reaction shown in Fig. 2a is quasi-reversible.

Various concentrations of DTPA (1–3 mM) were added to the cerium solution and the colour of the solution changes after adding 3 mM DTPA, the colour changes from deep yellow to light yellow. The ionic strength was strictly kept constant, since the change in the rate constant could be due to the small changes in the ionic strength. Sodium hydroxide was used to adjust the pH of the solution

**Fig. 1** Cyclic voltammograms for platinum electrode in: (a) 0.1 M  $\text{Ce}(\text{SO}_4)_2$  solution in 1 M  $\text{H}_2\text{SO}_4$  at a scan rate of  $100 \text{ mVs}^{-1}$  (b) at various scan rates: 20, 50, 100, 150 and  $200 \text{ mVs}^{-1}$  (c) Plot of peak current vs. square root of scan rate for voltammogram of Ce  $(\text{SO}_4)_2$  on Pt-electrode



to 4.5. Ce(IV)–DTPA complex provide better results at the pH 4.5 than the Ce(IV)–EDTA complex as shown in Fig. 2. Glentworth et al. [19] studied the kinetics of lanthanide polyaminopolycarboxylic acid complex ions, claiming that the rate of exchange depends on the pH of Ce–DTPA and on the concentration of Ce–DTPA complex. The reason is that the ligands may be considered to be electrostatically bonded to the metal ion and it is probable that the carboxylate group is unstable, i.e. there is a continuous breaking and reforming of the bonds. The unstable carboxylate group will be vulnerable to attack by protons

and the stability of the ligand will be increasingly reduced by successive protonation of the carboxylate group. Rao [22] studied the kinetics of EDTA, DTPA and its analogues by Ce(IV) in sulphuric acid medium using spectrophotometric methods. No electrochemical study is presented for Ce–DTPA. Rao confirmed that the rate constant depends on the nature of amino groups i.e. tertiary > secondary > primary. This implies that a ligand like EDTA will be less vulnerable to attack by an oxidizing agent like Ce(IV) in sulphuric acid than DTPA. Therefore the Ce(IV)–DTPA complex will be more stable and more

**Fig. 2** Cyclic voltammogram of a 0.1 M Ce(SO<sub>4</sub>)<sub>2</sub> solution in 1 M H<sub>2</sub>SO<sub>4</sub> at a platinum electrode. With (a) 0.03 M DTPA at a scan rate of 100 mVs<sup>-1</sup> (b) at various scan rates: 20, 50, 100, 150 and 200 mV s<sup>-1</sup> in (c) 0.1 M of Ce(SO<sub>4</sub>)<sub>2</sub>, Ce(IV)–EDTA and Ce(IV)–DTPA. (d) Randles plot for the redox reaction of Ce(IV)–EDTA. (e) Randles plot for the redox reaction of Ce(IV)–DTPA

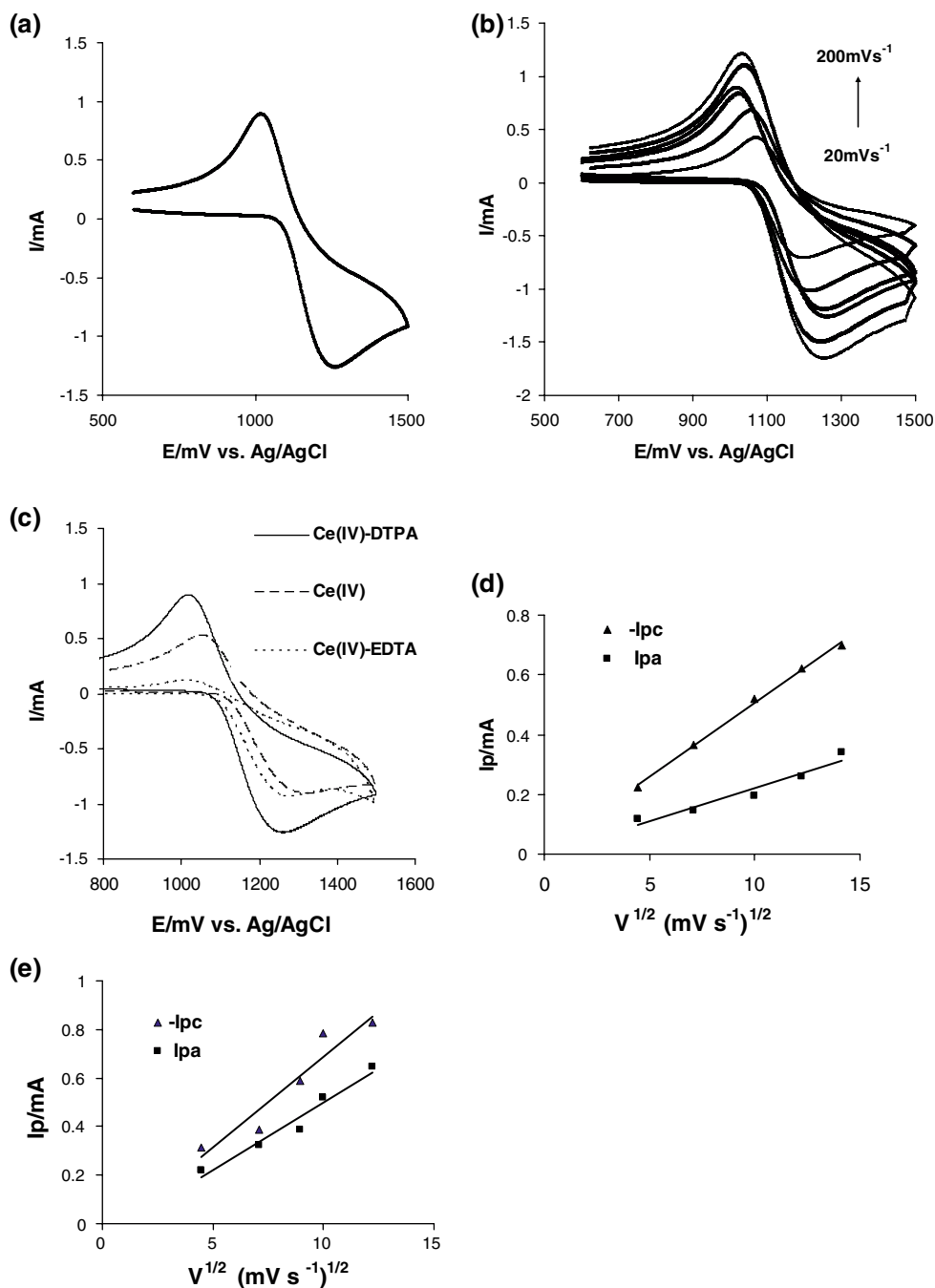


**Table 1** Cyclic voltammogram data for different electrolytes using a platinum electrode

Electrolyte	Diffusion coefficient $10^6 D/\text{cm}^2 \text{ s}^{-1}$		Electron coefficient ( $\alpha$ )		Standard rate constant $10^4 k^0/\text{cm}^{-1}$	
	This work	Literature values	This work	Literature values	This work	Literature values
Ce(IV)	2.4	3.20 <sup>a</sup> [21]	0.31	–	1.6	1.9 [21]
Ce(IV)–EDTA	1.3	–	0.36	–	1.9	1.8 <sup>b</sup> [18]
Ce(IV)–DTPA	1.1	–	0.42	–	3.1	–
Fe(III)	2.3	3.24 <sup>c</sup> [25] 7.6 [26]	0.39	–	2.1	3.25 [25] 2.87 <sup>c</sup> [26]
Fe(III)–EDTA	1.9	1.50 <sup>d</sup> [25]	0.48	0.49 [27]	2.6	1.9 <sup>e</sup> [27]
Fe(III)–DTPA	0.28	0.20 [25]	0.51	–	2.3	156 [25]

<sup>a</sup> Diffusion coefficient of Ce(IV) at Au-electrode =  $0.32 \times 10^{-5} \text{ cm}^2 \text{ s}^{-1}$  [21]

<sup>b</sup> The rate constant ( $k$ ) of Ce(IV)–EDTA in 0.1 M KCl =  $1.86 \text{ s}^{-1}$  [18]

<sup>c</sup> The rate constant ( $k$ ) of Fe(III) at Diamond-electrode =  $2.87 \times 10^{-3} \text{ s}^{-1} \text{ cm}$  [26]

<sup>d</sup> Diffusion coefficient of Fe(III) at Pt-electrode =  $1.50 \times 10^{-6} \text{ cm}^2 \text{ s}^{-1}$  [25]

<sup>e</sup> The rate constant ( $k$ ) of Fe(III)–EDTA at Au-electrode =  $1.9 \text{ cm}^2 \text{ s}^{-1}$  [27]

suitable for redox flow batteries than the Ce(IV)–EDTA system.

A plot of the peak current ( $i_p$ ) for the oxidation and reduction processes versus square root of scan rate ( $v^{1/2}$ ) in Fig. 2d and e shows the dependence of peak current for the oxidation and reduction process of the Ce(IV)–DTPA complex; the peak current are a linear function of the potential scan rate, confirming that these processes are limited by the surface processes. It also proves that the Ce(IV)–DTPA complex is a quasi-reversible redox process within the potential range and is controlled by diffusion limited reaction. Figure 2d shows a large current separation between the anodic and cathodic lines indicating faster kinetics for the reduction process than the oxidation process for the Ce(IV)–EDTA complex. In contrast Fig. 2e illustrates that the anodic “line” and cathodic “line” is close together and having similar slopes, indicative of relatively comparable electron transfer rates. However the Ce(IV)–EDTA complex is slightly limited by the surface processes and a poor linear response is achieved as shown in Fig. 2d. Figure 2c shows an overlap of the three voltammograms of the redox behaviour of Ce(IV) in sulphuric acid, the Ce(IV)–EDTA complex and the Ce(IV)–DTPA complexes respectively. The anodic and cathodic peak currents of the Ce(IV)–DTPA complex is higher than the corresponding currents for the Ce(IV)–EDTA complex and Ce(IV) at the same concentration, indicating a faster electron transfer at the platinum working electrode for the former. This enhanced electron transfer compared to the other complexes is also supported by the electron transfer coefficient ( $\alpha$ ) for this reaction.

The rate constant, diffusion coefficient and electron coefficient for Fe(III), Fe(III)–EDTA and Fe(III)–DTPA are shown in Table 1. The values of ( $k$ ) were obtained from the plot of  $\ln i$  vs potential ( $E-E^0$ ), and found to be ( $k$ ) =  $2.1 \times 10^{-4} \text{ cm}^2 \text{ s}^{-1}$  Fe(III), Fe(III)EDTA

( $k$ ) =  $2.6 \times 10^{-4} \text{ cm}^2 \text{ s}^{-1}$  and Fe(III)DTPA ( $k$ ) =  $2.3 \times 10^{-4} \text{ cm}^2 \text{ s}^{-1}$ . The value of ( $\alpha$ ) were also obtained from the same plot of  $\ln i$  vs potential ( $E-E^0$ ), and found to be ( $\alpha$ ) = 0.39 Fe(III), ( $\alpha$ ) = 0.48 Fe(III)EDTA and ( $\alpha$ ) = 0.51 Fe(III)DTPA as shown in Table 1. In comparison the Fe(III)EDTA complex species have a larger ( $k$ ) value than the uncomplexed species, meaning that the reaction will be faster when the EDTA and DTPA complexes are used rather than the uncomplexed species of Fe(III).

### 3.2 Rotating disc voltammetry

The voltammograms of rotating disc electrochemistry was shown in Fig. 3 and obtained at rotation rates between 200 and 4000 rpm. The limiting current results were plotted versus the square root of rotation rate as illustrated in Fig. 3c, a linear relationship been found between the square root of rotation rate and the limiting current. This demonstrate that Ce(IV)–DTPA reaction obeys the Levich equation below [23]

$$i_L = (0.620) nFA D^{2/3} v^{-1/6} \omega^{1/2} C \quad (1)$$

where  $i_L$  is the Levich current,  $n$  is the number of electrons,  $F$  is the Faraday constant.  $A$  is the electrode area (in  $\text{cm}^2$ ),  $D$  is the diffusion coefficient (in  $\text{cm}^2 \text{ s}^{-1}$ ),  $\omega$  is the rotation rate (radians/s) and  $\nu$  is the kinematic viscosity ( $\text{cm}^2 \text{ s}^{-1}$ ), and  $C$  is concentration ( $\text{mol cm}^{-3}$ ). The values of the diffusion coefficient obtained from Fig. 3c are shown in Table 1. A plot of  $\ln i$  vs potential ( $E-E^0$ ) were constructed as shown in Fig. 3d and a straight line plot was obtained with a linear regression of 0.9934.

The rate constant ( $k$ ) was calculated from the Levich plot and found to be in the range  $1.6\text{--}3.1 \times 10^{-4} \text{ cm}^2 \text{ s}^{-1}$ , and is in good agreement with those found by earlier researchers [18, 20] as listed in Table 1. Therefore the

process is diffusion controlled. The diffusion coefficient of the uncomplexed Ce(IV) in 1 M H<sub>2</sub>SO<sub>4</sub>, calculated from the slope of the straight line, was found to be  $2.4 \times 10^{-6}$  cm s<sup>-1</sup> as shown in Table 1. This is lower than the value of  $3.2 \times 10^{-6}$  cm s<sup>-1</sup> found in the literature [16, 17, 20]. A plot of  $i_L$  vs.  $w^{1/2}$  gave a straight line with slope proportional to  $D^{2/3}$ . For a quasi-reversible process, the peak potential  $E_p$  is a function of scan rate, the difference between  $E_p$  and formal potential  $E^o$ , being related to the standard rate constant. The peak current may also be expressed as in Eq. 2 [24].

$$i_p = (0.227) nFAc k \exp[-(\alpha nF/RT)](E - E^o) \quad (2)$$

A plot of  $\ln i$  vs  $(E - E^o)$ , determined at different scan rates, should have a slope of  $-(\alpha nF/RT)$  with the intercept proportional to  $(k)$ . The rate constant for the uncomplexed Ce(IV) in 1 M H<sub>2</sub>SO<sub>4</sub> was calculated to be  $1.6 \times 10^{-4}$  cm s<sup>-1</sup> as shown in Table 1. This is a reasonable agreement with the value  $1.9 \times 10^{-4}$  m s<sup>-1</sup> found in the literature [20].

No kinetic and electrochemical data were available in the literature for the Ce(IV)–DTPA system for use in redox flow battery systems. Therefore the kinetics of uncomplexed Ce(IV) and Ce(EDTA) are the only points of reference, as shown in Table 1. The Fe(III) EDTA and Fe(III)(DTPA) systems were also evaluated and used as a further point of reference. In comparison the Ce(IV)–DTPA complex species have a larger  $(k)$  value than the uncomplexed species, meaning that the reaction will be faster when DTPA is used rather than EDTA and uncomplexed species (Ce(IV)).

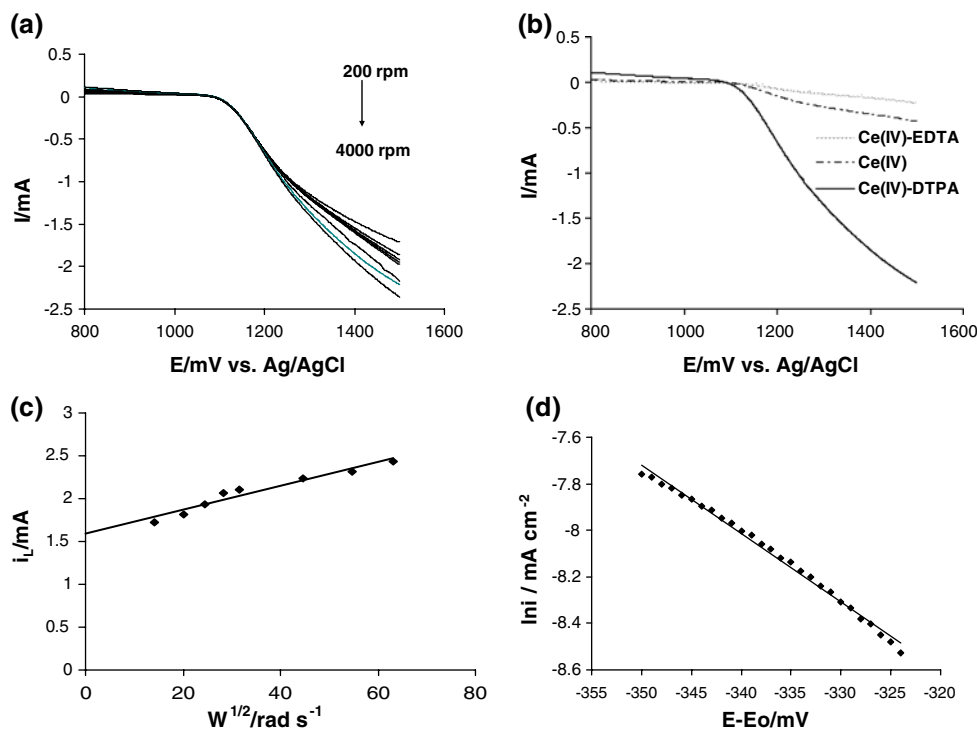
## 4 Conclusion

The electrochemical behaviour of the complexation of cerium(IV) with EDTA and DTPA was studied using both cyclic voltammetry (CV) and rotating disc electrochemistry (RDE).

The results for cyclic voltammetry study of Ce(IV)–DTPA illustrate a quasi-reversible 1e- transfer reaction electrode process on platinum. A potential separation ( $\Delta E_p$ ) of greater than 59 mV was observed; this was dependent on scan rate. The Ce(IV)–DTPA complex at various scan rates gave a linear correlation between the peak current ( $E_p$ ) and square root of scan rate, showing that the kinetics of the overall process was diffusion-controlled.

RDE results also provided information about the electron transfer mechanism in the absence of any mass restriction. The kinetic tests also showed that the Ce(IV)–EDTA redox reaction at platinum was a relatively slow heterogeneous reaction. The electrochemical studies of the Ce(IV) in the presence of EDTA show irreversible behaviour. EDTA was therefore found not to be a suitable ligand for use in electrolytes of RFB. In the Ce(IV) uncomplexed species the results show a quasi-reversible electrochemical behaviour with a lower electron transfer rate constant. The electrochemical study of Ce(IV), Ce(IV)–EDTA and Ce(IV)–DTPA at the platinum electrode indicated that the highest  $k$  value was between  $1.6$  to  $3.1 \times 10^{-4}$  cm s<sup>-1</sup> and the diffusion coefficients between  $1.1$  to  $2.4 \times 10^{-6}$  cm s<sup>-1</sup>. The Ce(IV)–DTPA complex species have a higher electron transfer rate constant than

**Fig. 3** Hydrodynamic voltammograms of a 0.1 M Ce(SO<sub>4</sub>)<sub>2</sub> solution in 1 M H<sub>2</sub>SO<sub>4</sub> at a Platinum electrode with (a) 0.03 M DTPA at various rotation rates: 200, 400, 600, 800, 1000, 2000, 3000 and 4000 rpm (b) in Ce(SO<sub>4</sub>)<sub>2</sub>, Ce(IV)–EDTA and Ce(IV)–DTPA at a rotation rate of 1000 rpm. (c) Plot of Levich current vs square root of rotation rate for the (d) a plot of  $\ln i_p$  vs. potential  $(E - E^o)$



the Ce(IV)–EDTA complex and uncomplexed species Ce(IV), respectively. This indicates that the rate of electron transfer was fast. An all Cerium redox couple in which the DTPA ligand will be used as an electrolyte for the redox flow battery system has an advantage over the Ce–EDTA or Ce(IV) uncomplexed species. Hence the suggestion is that a redox flow battery employing the Ce(IV)–DTPA complex as the positive active species will have a high voltage efficiency and will satisfy an important requirement for a redox flow battery electrolyte.

**Acknowledgments** The authors acknowledge financial support by the National Research Foundation (NRF), South Africa and the Tertiary Education Support Program (TESP) of the Electricity Supply Commission (ESKOM), South Africa.

## References

1. Rychcik M, Skyllas-Kazacos M (1988) *J Power Sources* 22:59
2. Thaller LH (1979) In: NASA TM-79143, National Aeronautics and Space Administration US Department of Energy
3. NASA TM-79067 (1977) National Aeronautics and Space Administration, US Department of Energy
4. Liu Y, Xia X, Liu H (2004) *J Power Sources* 130:299
5. Reid MA, Thaller LH (1980) NASA Tech Membr 809289:1471
6. Sum E, Skyllas-Kazacos M (1985) *J Power Sources* 15:179
7. Tsuda I, Nozaki K, Sakuta K, Kurokawa K (1997) *Sol Energy Mater Sol Cells* 47:101
8. Hasegawa K, Kimura A, Yamamura T, Shiokawa Y (2005) *J Phys Chem Solids* 66:593
9. Yamamura T, Watanabe N, Shiokawa Y (2006) *J Alloy Comp* 408:1260
10. Skyllas-Kazacos M, Grossmith F (1987) *J Electrochem Soc* 34:2950
11. Kazacos M, Skyllas-Kazacos M (1989) *J Electrochem Soc* 136:2759
12. Doria J, De Andres MC, Armenta C (1985) *Proc 9th Solar Energy Soc* 3:1500
13. Chen YWD, Santhanam KSV, Bard AJ (1981) *J Electrochem Soc* 128:1460
14. Fang B, Iwasa S, Wei Y et al (2002) *Electrochim Acta* 47:3971
15. Paulenova A, Creager SE (2002) *J Power Sources* 109:431
16. Pletcher D, Valder E (1988) *Electrochim Acta* 33:499
17. Wei Y, Fang B (2005) *J Appl Electrochem* 35:561
18. Abbaspour A, Mehrgardi MA (2005) *Talanta* 67:579
19. Glentworth P, Wiseall B, Wright CL et al (1968) *J Inorg Nucl Chem* 30:967
20. Kiekens P, Steen L, Donche H et al (1981) *Electrochim Acta* 26:841
21. Pletcher D, White JCP (1992) *Electrochim Acta* 37:575
22. Rao GN (1970) *Indian J Chem* 8:328
23. Bard AJ, Faulkner LR (2001) *Electrochemical methods fundamentals and applications*, 2nd edn. John Wiley & Sons, New York
24. Zanello P (2003) *Inorganic electrochemistry theory, practice and application*. The Royal Society of Chemistry, Cambridge
25. Murthy ASN, Srivastava T (1989) *J Power Sources* 27:119
26. Zang JB, Wang YH, Zhao SZ, Bian LY, Lu J (2007) *Diamond Relat Mater* 16:16
27. Cai C, Mirkin MV (2006) *J Am Chem Soc* 127:171